

SUBCHANNEL MODELLING CAPABILITIES OF RELAP5-3D[®] FOR WIRE-SPACED FUEL PIN BUNDLE

C. CIURLUINI¹, V. NARCISI¹, F. GIANNETTI¹, P. LORUSSO², M. TARANTINO², G. CARUSO¹

¹DIAEE – Nuclear Section, “Sapienza” University of Rome, Rome, Italy

²ENEA, Department of Fusion and Technology for Nuclear Safety and Security, Camugnano, BO, Italy

Email contact of corresponding author: cristiano.ciurluini@uniroma1.it

Abstract

A computational campaign was carried out at the Department of Astronautical, Electrical and Energy Engineering (DIAEE) of “Sapienza” University of Rome, aiming at the assessment of RELAP5-3D[®] capabilities for subchannel analysis. More specifically, the investigation involved LBE-cooled wire-spaced fuel pin bundle, by comparing simulation outcomes with experimental data coming from NACIE-UP facility, hosted at ENEA Brasimone Research Center. The thermal-hydraulic nodalization of the facility was developed with a detailed subchannel modelling of the Fuel Pin Simulator (FPS). Three different methodologies for the subchannel simulation were investigated, increasing step by step the complexity of the thermal-hydraulic model. In the simplest approach, the subchannels were modelled one by one. In addition, mass transfer between them was considered thanks to multiple cross junction components, realizing the hydraulic connection between adjacent subchannels. In this case, mass transfer depends on pressure gradient and hydraulic resistance only, ignoring the turbulent mixing promoted by the wire wrapped. Simulation results were not satisfactory, and an improvement was introduced in the second approach. In this case, several control variables calculate at each time step the energy transfer between adjacent control volumes associated to the turbulent mixing, induced by the wires. This energy is transferred using “ad hoc” heat structures, where the boundary conditions are calculated by the control variables. The present model highlighted good capabilities in the prediction of the radial temperature distribution within the FPS, considerably reducing disagreement with experimental data. Finally, the influence of the radial conduction within the fluid domain was assessed, introducing further heat structures. Although this most complex model provided the best estimation of the experimental acquisition, the improvements given by the radial conduction were not so relevant to justify the correspondent increase of the computational cost.

1. INTRODUCTION

One of the most challenging issues of this century is the fight against climate change. The need to reduce CO₂ emissions has dramatically increased the interest in such power plants able to produce a large amount of electric power while lowering (or avoiding) the release of greenhouse gases. Within this framework, the fission nuclear reactors can play a fundamental role. In particular, the Generation IV (GEN IV) power plants, with their innovative designs, can provide solutions to achieve the following fundamental goals: sustainability, economics, safety and reliability, proliferation resistance and physical protection, [1]. Among the other, one of the most promising technologies is represented by the Lead Fast Reactors (LFRs). They foresee the adoption of lead or lead-bismuth eutectic (LBE) as primary coolant, ensuring several advantages in terms of reactor performances and safety. Indeed, this fluid is characterized by a very high boiling temperature and non-hazardous reactions with both air and water. Although, to accomplish the GEN IV policy goals (i.e., enhanced actinide management, nuclear power plant economic competitiveness) a reliable fuel operation at high-burnup and high-power density must be guaranteed. Consequently, LFRs are characterized by high fuel and cladding temperatures, [2]. In these conditions, some concerns arise related to the interaction of the liquid metal with the reactor structural materials. Considering all these aspects, an affordable core design must include an effective thermal-hydraulic characterization of the fuel bundle at a subchannel level.

Throughout the last decades, many codes were developed to fulfil this purpose, some of them specific for liquid metal applications. SUPERENERGY II, [3], MATRA-LMR, [4], and COBRA-LM, [5], refer to Sodium-cooled Fast Reactors (SFRs), while ANTEO+, [6], and SACOS-PB, [7], are used for LFRs. In a subchannel analysis, the fuel assembly is divided in coarse meshes, each one constituted by a single fuel rod and the correspondent coolant volumes. One-dimensional conservation equations are solved for the fluid along flow (axial) direction. In addition, mass, momentum and energy exchanges between adjacent subchannels are considered. They are due to cross flow and mixing and are simulated by using constitutive relations which couple

the conservative equations belonging to adjacent subchannels. SubChannel Thermal-Hydraulic (SCTH) codes, such as the ones named above, are mainly ad hoc fast-running numerical tools developed to study specific problems, in terms of assembly geometry (e.g., hexagonal wire-wrapped), fuel configuration (e.g., solid cylindrical pin) and coolant (i.e., sodium or lead). When one of these pre-set features is breached, the correspondent SCTH code is no more suitable. This strongly limits their applicability to study new design solutions.

To study such original geometries, an alternative option could be the usage of full Computational Fluid Dynamics (CFD) codes. In the last years, several investigations have been performed with these tools, [8][9][10][11][12]. Numerical calculations focused on the 3D thermal-hydraulic phenomena that the one-dimensional subchannel codes are not able to evaluate (e.g., vortex, boron concentration). CFD codes can handle any kind of assembly geometry, fuel configuration and coolant. The main drawback is that they require a very high spatial resolution near the structural walls (i.e., large number of meshes), dramatically increasing the computational cost.

Within this framework, a good compromise can be represented by the adoption of best-estimate System Thermal-Hydraulic (STH) codes. This category of numerical tools is not affected by pre-set limitations, in contrast with SCTH codes, allowing the modelling of complex fuel geometries with a large choice of coolant media. They are not able to catch the 3D flow details characterizing a CFD simulation, but they are suitable to investigate the system behaviour in transient and accidental conditions. Referring to computational cost, STH calculations are more expensive than SCTH ones, but drastically cheaper than CFD simulations. However, the STH code capabilities with respect to subchannel analysis must be verified and evaluated. In literature, numerical analyses adopting this approach are already present, [13]. Although, they refer to sodium cooled fast reactor applications.

The scope of the paper is to discuss a computational activity carried out at the Department of Astronautical, Electrical and Energy Engineering (DIAEE) of “Sapienza” University of Rome. It focuses on the STH code RELAP5-3D[®], [14]. More specifically, the investigation involved LBE-cooled wire-spaced fuel pin bundle, by comparing simulation outcomes with experimental data coming from NACIE-UP facility, hosted at ENEA Brasimone Research Center.

2. NACIE-UP: FACILITY OVERVIEW AND EXPERIMENTAL CAMPAIGN

Within the framework of HORIZON 2020 Safety Assessment of Metal cooled reactor (SESAME) project, a test campaign was performed with the NACIE-UP (NATURAL Circulation Experiment- UPgraded) facility, hosted at the ENEA Brasimone Research Centre, [15]. In the paper, such experimental results are compared with the numerical outcomes of the RELAP5-3D[®] system code in order to evaluate its capability with respect to subchannel analysis. For this, a full description of the facility is out of scope (for detailed information, refer to [15]). In the following, only the main features of the experimental setup are recalled.

It consists in a rectangular primary circuit where flows LBE, as shown in FIG. 1a. The vertical sections are nearly 8 meters high, while the horizontal pipelines have a length of 2.4 meters. The Fuel Pin Simulator, replacing the reactor core, is installed at the bottom of the riser. Instead, the water/liquid metal Heat eXchanger (HX), acting as system heat sink, is installed at the top of the downcomer. The height difference between the thermal centres of these two components is almost 5.5 meters. This parameter is of capital importance in the transients involving natural circulation. During normal operations, the LBE flow is enhanced through the injection of Argon (Ar). This occurs thanks to a nozzle located downstream with respect to the FPS. The Ar injection line is evidenced in green in FIG. 1a. Once introduced in the system, the gas is then separated from the LBE stream in the expansion vessel situated at the riser top. The facility is highly instrumented. Several thermocouples are placed in relevant positions along the flow path to fully characterize the liquid metal temperature field at system scale. Moreover, a prototypical flowmeter is inserted in the lower horizontal pipe to acquire the LBE mass flow. The sensor detailed list is provided in [15], together with an indication of the related measurement uncertainties.

For the purpose of the current simulation activity, the most important component is the fuel bundle simulator. For it, the main geometrical parameters are reported in Table 1. Each pin is electrically heated and wrapped with a wire acting as spacer. Their total height is 2 meters. An initial non-active region (500 millimetres) allows to obtain a fully developed flow at the inlet of the active one, which extends for further 600 millimetres. Within this length, three elevations are instrumented: 38, 300 and 562 mm, considering $z = 0$ at the beginning of the active zone. They are named section A, B, and C, respectively. At each quote, both wall and fluid bulk

temperatures are acquired. The selected pins, equipped with wall-embedded thermocouples, as well as the chosen channels, provided with bulk thermocouples, are shown in FIG. 1b.

During the experimental campaign of 2017, three Fundamental Tests (FT) were performed at the NACIE-UP facility, [15]. The main goal was the evaluation of the circuit thermal-hydraulic behaviour associated to a power and/or mass flow transient. A special focus was given to the fuel assembly cooled by heavy liquid metal. The final purpose of the campaign was understanding the performances of such system during a Loss of Flow Accident (LOFA). In each FT, the loop started from steady state conditions. Then, a transition was imposed, either in terms of power or mass flow or both. When the system reached a new steady state, the test was concluded. A brief description of each FT is provided in Table 2. In order to perform the code-to-experiment comparison, such test campaign offers the precious opportunity to assess the subchannel modelling in both steady state and transient conditions. Initially, the first experiment was selected. In the future developments of the activity, also the others will be considered.

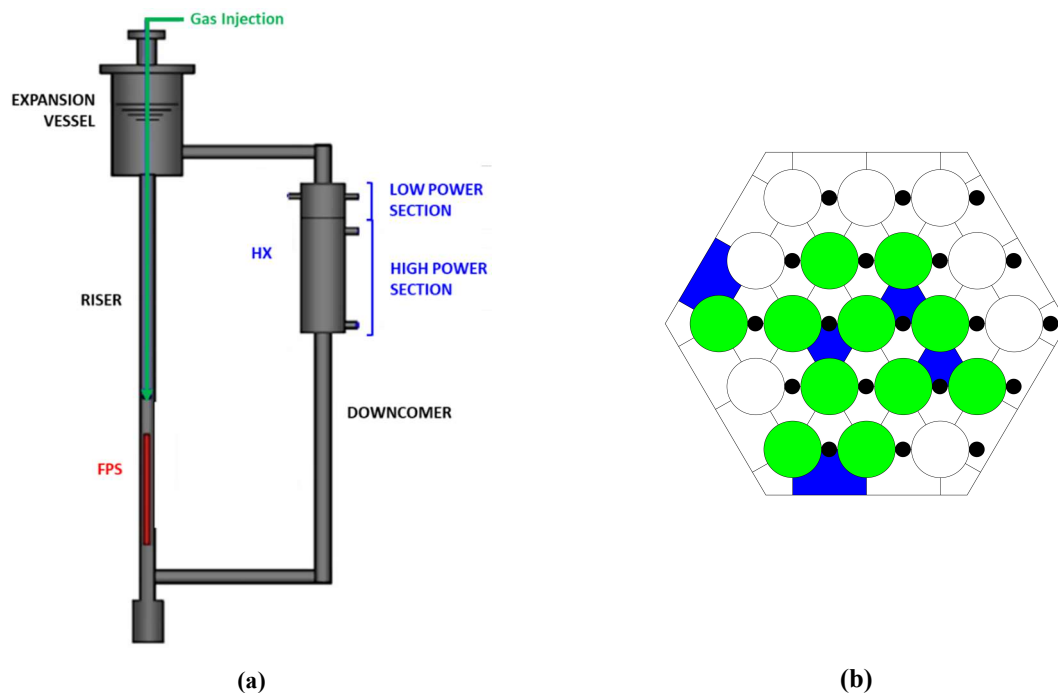


FIG. 1. NACIE-UP facility: a) primary circuit; b) FPS with instrumented pins and subchannels, [15].

Table 1. FPS main geometrical parameters, [15]

Parameter	Unit	Value
Pin number	-	19
Pin OD	mm	6.55
Pin Pitch	mm	8.4
Wire OD	mm	1.75
Wire Vertical Pitch	mm	262
LBE flow area	mm ²	654.4
Hexagonal wrapper apothem	mm	19.67

Table 2. Fundamental Tests performed at NACIE-UP facility: transient boundary conditions, [15]

Test	Description
FT1	<u>Gas-lift transition</u> : gas flow reduces from 20 N l min ⁻¹ (rated value) to 10 N l min ⁻¹ , while FPS power and HX feedwater flow are maintained at 50 kW and 10 m ³ h ⁻¹ (at 443 K and 1.6 MPa).
FT2	<u>Power transition</u> : FPS power reduces in 50 s from 100 kW to 50 kW, while gas injection and HX feedwater flow are kept at 18 N l min ⁻¹ and 6.6 m ³ h ⁻¹ (at 443 K and 1.6 MPa).

FT3	<u>Protected Loss of Flow Accident (PLOFA)</u> : FPS power reduces in 10 s from 100 kW to 10 kW, Argon flow decreases from 20 N l min ⁻¹ to 0 N l min ⁻¹ in 1 s, while HX feedwater flow is kept at 10 m ³ h ⁻¹ (at 443 K and 1.6 MPa).
------------	---

3. RELAP5-3D[®] FPS SUBCHANNEL MODELLING

The DIAEE of “Sapienza” University of Rome was already involved in simulation activities related to the NACIE-UP facility, [16]. Within this framework, a complete RELAP5-3D[®] model of the primary circuit was developed. The purpose is to evaluate the code capability in simulating the loop transient behaviour at a system level. For this, the FPS was modelled as a single equivalent pipe characterized by lumped parameters (total bundle flow area and mass flow, bundle hydraulic diameter, etc.). Starting from this version, the nodalization scheme was improved by including a detailed subchannel modelling of the fuel bundle simulator, shown in FIG. 2a. In the following, the latter is widely discussed. Instead, for a comprehensive description of the rest of the nodalization scheme, refer to [16].

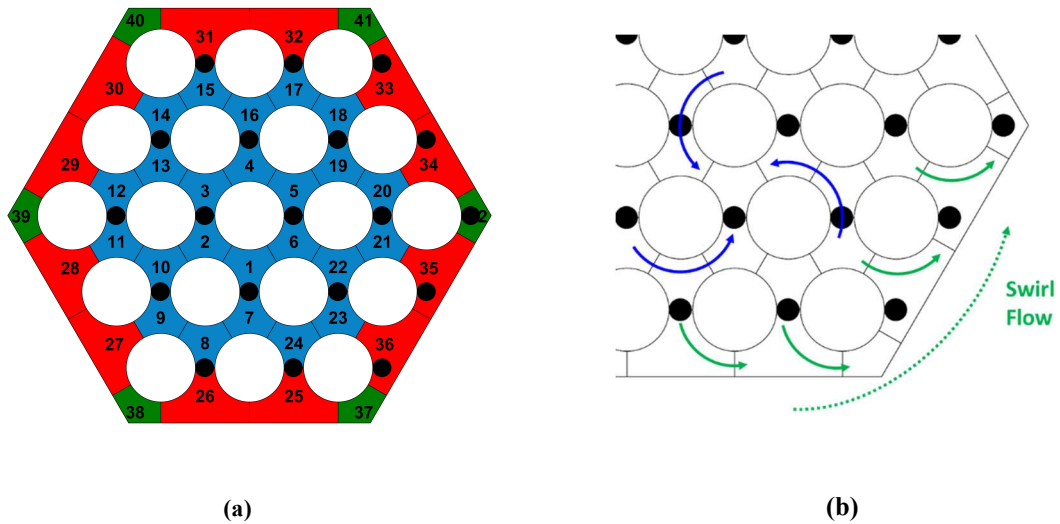


FIG. 2. RELAP5-3D[®] FPS improved modelling: a) subchannel division (blue: interior; red: edge; green: corner) and numbering; b) ‘swirl’ flow in interior subchannels (blue arrows) and edge/corner subchannels (green arrows).

The rationale behind the FPS modelling follows the lessons learned from [17] and [13]. The presence of the wires wrapped to the pins leads to an increase in the bundle pressure drops and enhances the cross flow among adjacent channels by adding a swirl contribute. Indeed, when the axial flow meets the wire-wrap, it starts to swirl around the pin following the wire-wrap helical shape. These two phenomena must be properly simulated while developing the RELAP5-3D[®] model. To do it, several aspects must be carefully considered: **i)** the FPS geometrical scheme; **ii)** the cross-flow model, to account for the lateral mass exchange between subchannels; **iii)** the wire-wrap induced turbulent mixing model, generating mass and energy transfer among adjacent channels; **iv)** the fluid conduction model, in both axial and radial directions. To separately evaluate their impact on the simulation outcomes three different FPS models were tested against experimental results. The first contains the improved geometrical scheme for the FPS and the cross-flow model only (**‘cmo’**). In the second, the wire turbulent mixing (**‘wtm’**) was added. Finally, also the fluid thermal conduction (**‘ftc’**) was included in the input deck.

Referring to the geometrical scheme, the overall fuel bundle simulator was divided into 42 subchannels, grouped in three main categories: interior (24), edge (12) and corner (6) subchannels, respectively blue, red and green in FIG. 2a. They are characterized by a different thermal-hydraulic behaviour. For this, each channel was modelled with a dedicated pipe component. The axial discretization foresees ten Control Volumes (CVs) distributed between the entry non-active region (4), the active length (5) and the unheated exit region (1). A sensitivity was performed by increasing the number of axial meshes (i.e., computational time) but no sensible differences were detected in the simulation results. Thus, the aforementioned vertical nodalization was consolidated as reference. To account for the increased pressure drops due to the wire presence, it was used the

theory developed by Cheng and Todreas for liquid metal fuel bundle, [17]. So far, it was used their 1986 model. Although, in recent years, the two scientists updated their results, as reported in [18]. In the future development of the activity, it is planned to upgrade the current input deck considering the newly developed correlations. Cheng and Todreas divide the overall assembly in two regions: interior and edge. Within the gap between two adjacent interior rods, the swirl flow periodically turns around following the axial coordinate (see FIG. 2b). Thus, the wire-induced swirl mixing associated to these channels can be simulated as an enhanced eddy diffusivity. Instead, referring to the edge region, the wire global effect is to transport fluid in the azimuthal direction, if cylindrical coordinates are assumed for the assembly. In this case, the swirl flow can be represented by a constant transverse flow throughout all the correspondent gaps (see FIG. 2b). Considering that edge and corner subchannels have different geometrical shape, Cheng and Todreas developed three different friction factor correlations, starting from the ones for a bare bundle, [17]. Such models cover all the flow regimes occurring during liquid metal fast reactor transients, i.e., laminar, transition and turbulent. Since RELAP5-3D[®] gives the user the possibility to implement ad-hoc Reynolds-dependent friction factor correlations, they were introduced in the input deck, differentiated for each subchannel type. The procedure is described in [19].

Regarding the cross-flow model, the coupling between adjacent subchannels was realized by means of multiple junction components. They group the overall 600 cross junctions needed to connect each pair of channels at the different axial locations (10 per pair, as discussed above). In ‘**cmo**’ model, where wire turbulent mixing is ignored, the mass transfer depends on pressure gradient and hydraulic resistance only. To properly simulate them, k-loss coefficients were entered in the RELAP5-3D[®] input deck and associated to the cross junction components. They were evaluated by using the formulas available in [20], as described in [21].

For what concerns the wire-induced turbulent mixing, introduced starting from ‘**wtm**’ model, the procedure to implement it in the RELAP5-3D[®] input deck is fully discussed in [13]. Even in this case, different approaches were considered for interior and edge regions. For an inner channel, at any axial location, when the lateral mass flow balance is performed at the correspondent gaps, both inflow and outflow contributions are present (see FIG. 2b). Each element is proportional to the axial mass flux in the related adjacent subchannel. Since the axial mass flow is nearly the same in all the inner channels, the net lateral flow is almost null. As a result, in the interior region, the wire turbulent mixing affects the energy but not the mass conservation equation. This lateral thermal transfer can be calculated by using formulas provided in [13]. Instead, as discussed above, the edge region is characterized by a swirl flow circulating along the overall assembly-perimeter, as shown in FIG. 2b. Consequently, in this case, the wire presence influences both the thermal and mass balances, flattening the temperature distribution in the assembly duct. The effect of the swirl flow on the edge channel energy equation can be quantified and simulated through relations reported in [13]. Such power terms, differentiated for each channel and each axial mesh (420 in total), are computed in the RELAP5-3D[®] model thanks to a set of more than one thousand control variable components. Then, they are associated to the corresponding control volumes by means of ad hoc Heat Structure (HS) components. They are featured by negligible thickness, a heat transfer surface consistent with the CV geometry, LBE thermal conductivity and a negligible heat capacity (to avoid alterations of the system thermal inertia).

Finally, the fluid thermal conduction model was inserted in the last input deck (‘**ftc**’). RELAP5-3D[®] was originally developed to simulate safety-relevant transient scenarios belonging to Light Water Reactors, [14]. When it comes to water, energy exchange due to conduction is negligible with respect to convection. For this, RELAP5-3D[®] lacks a model accounting for such heat transfer mechanism. Nevertheless, it can significantly affect thermal problems involving liquid metals. Studies present in literature, [22], propose the adoption of a modified Peclet number (Pe^*) as reference parameter to assess the relative importance of conduction along axial and radial directions. As discussed in [13][21], axial conduction never plays a significant role in the liquid metal thermal-hydraulic behaviour. Thus, it was neglected in the current work. Instead, radial conduction can moderately influence the transient characterized by low flow rate (e.g., FT2 and FT3). It was modelled by following the approach described in [13][19][21], i.e., adding ad hoc heat structure components to the RELAP5-3D[®] input deck. A dedicated HS was associated to each pair of hydraulically-connected channels at each axial location (600 in total). They are characterized by: a thickness equal to the distance between adjacent channel geometric centres; a heat transfer surface corresponding to the gap transverse area (limited to the axial mesh of interest); LBE thermal conductivity; a negligible heat capacity (to avoid alterations of the system thermal inertia). Moreover, to exclude the convective thermal resistance, a very high multiplicative factor was entered in the HS. For more details about the fluid thermal conduction model, refer to [19][21].

The electrically-heated pins were simulated by means of additional HSs, reproducing the actual rod geometry. The overall power is axially distributed according to the vertical nodalization of the active zone. Looking at the experimental results collected in [15], a small fraction of the total electric heating (i.e., 8%) is dissipated in the ‘theoretically’ unheated entry region. This aspect was maintained in the RELAP5-3D[®] model. Within fuel bundle, the fluid HTC was evaluated by using Westinghouse correlation, [23], the one ensuring the most reliable results in comparison with experimental data, [15]. Finally, heat structure components were also used to represent the test section thermal insulation. They account for the material inventories associated to the shell hexagonal duct and the outermost insulator layer. Constant environment temperature (285 K) and heat transfer coefficient ($3 \text{ Wm}^{-2}\text{K}^{-1}$) were imposed as boundary conditions on the HS external surface. The modelling features described in this last paragraph are in common for any RELAP5-3D[®] input deck (‘**cmo**’, ‘**wtm**’, ‘**fte**’).

4. SIMULATION RESULTS

To assess the RELAP5-3D[®] capabilities with respect to subchannel analysis, numerical outcomes must be compared with the experimental results. For this purpose, FT1 transient, described in Table 2, was selected. Calculations were run with a time step of 10^{-3} s. Simulations were carried out also with higher values of this parameter. Although, the Courant limit check performed by the code automatically reset the value to 10^{-3} s to allow the numerical convergence. Lower time steps were also tested but with negligible effects on the results. For LBE, the adopted thermophysical properties were the ones recommended by the Organization for Economic Co-operation and Development – Nuclear Energy Agency (OECD/NEA), [24]. They were implemented in RELAP5-3D[®] by DIAEE, [25]. A system scale analysis is not the goal of the paper. Hence, only the principal figures of merit related to the fuel bundle simulator are discussed in the following. The aim is to demonstrate that the system code is able to provide FPS inlet conditions consistent with the experimental data and to properly predict the global behaviour of the test section. The latter is the same for all the input decks adopted (‘**cmo**’, ‘**wtm**’, ‘**fte**’). The subchannel modelling influences only the temperature and flow distributions within the FPS. Instead, the component thermal balance (i.e. outlet temperature) depends on the input power and the inlet conditions (temperature and mass flow) provided by the rest of the circuit.

The gas rate reduction, indicated in Table 2, occurs from 1370 to 1400 s. Consequently, the LBE flow experiences a sudden drop followed by a stabilization at a slightly higher value, as shown in FIG. 3a. The system code is able to well predict the initial nominal value and the qualitative trend of this parameter during the transient evolution. However, it overestimates the flow steady value at the end of the test of about 4%. Such discrepancy falls within the error corresponding to the prototypical flowmeter measurements (5-7%) indicated in [15]. Referring to the mass flow step down, the code under predicts the magnitude of the variation of 0.1 kg/s (nearly 14% in relative terms). For what concerns the FPS temperatures, plotted in FIG. 3b, two main effects can be detected: the increase of the temperature difference between inlet and outlet sections and the rise of the average system temperature. The former is due to combined effect of the primary flow lowering while the FPS electrical power is kept constant. At the same time, the decrease of LBE flow rate modifies the thermal transfer within the HX. The primary fluid velocity reduces, as well as the correspondent heat transfer coefficient (HTC). Instead, at the secondary side, feedwater inlet conditions (temperature and mass flow, see Table 2) are maintained. The heat exchanger global HTC decreases and to remove the primary system power (kept constant in the FPS) the temperature difference between primary and secondary sides must rise. Being the secondary side conditions imposed, this is only possible with an increase of the primary system average temperature. RELAP5-3D[®] is able to well predict the discussed temperature transient both qualitatively and quantitatively.

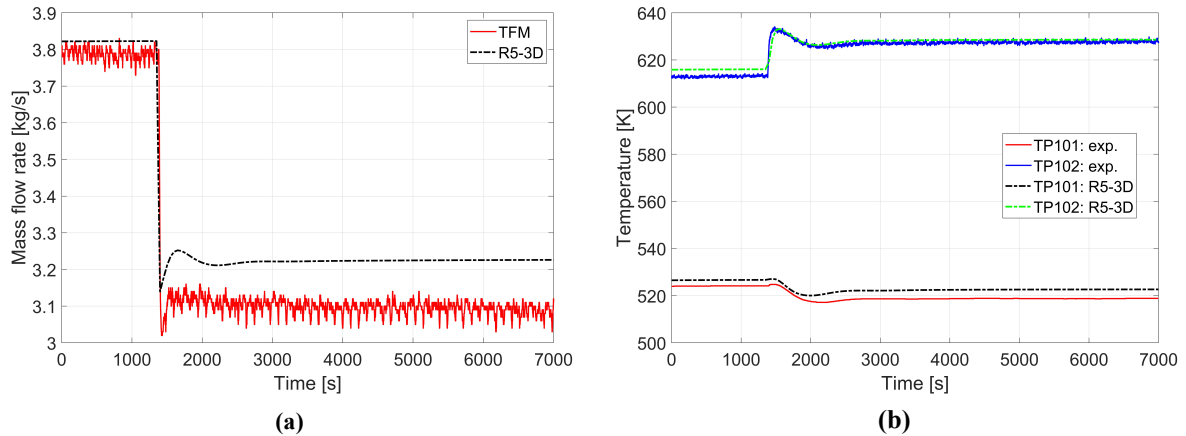


FIG. 3. Comparison between RELAP5-3D[®] and experimental results: a) LBE mass flow; b) FPS inlet and outlet temperatures.

Focusing on the FPS modelling, FIG. 4 collects all the channel temperatures needed to perform the comparison between RELAP5-3D[®] and the experiments. Test data are plotted together with error bars representing the measurement uncertainty (± 1 °C). The five instrumented channels are uniquely identified by their position with respect to the assembly center, assumed as zero (see FIG. 1b and FIG. 2a). Considering the increasing abscissa, they are sorted as following: 29 (-20.4 mm), 2 (-4.9 mm), 5 (4.9 mm), 22 (9.5 mm) and 26 (17.9 mm). All the three axial locations equipped with thermocouples are considered (i.e. sections A, B and C). Regarding section B, the temperature reading related to channel 26 is not reported since the corresponding sensor is out-of-service during the test campaign. Finally, the comparison is performed by taking into account both pre and post-transient steady state conditions, referring to 1000 and 6000 s in FIG. 3 and FIG. 5 respectively. The aim is to separately evaluate the impact of different phenomena on the simulation results and on their compliance to the experimental data. When only the cross-flow is considered (**'cmo'**) a partial mixing occurs in the bundle but it is not enough to flatten the temperature distribution as much as in the empirical observations. The introduction of the wire turbulent mixing has a deep impact on this aspect. The temperature profiles obtained as outcomes of **'wtm'** input deck are always able to qualitatively reproduce the empirical acquisitions. Instead, the introduction of the fluid thermal conduction, **'ftc'**, has a negligible effect on the simulation results. Along with the enhancement in code reliability, another important parameter to assess each model is based on the required computational time. The latter rises with the input deck complexity. It goes from 67 h for **'cmo'** to 70 h for **'wtm'** and 76 h for **'ftc'**. Only the first increase is justified by the improvement in the calculation outcomes. For what concerns the selected transient, even if characterized by a flow rate reduction, the influence of the radial conduction is negligible. Although, an ultimate judgement on the importance of such phenomenon on the LFR transient behaviour can be formulated only after the analysis of FT3, where the complete transition from gas-lift to natural circulation is foreseen. From a quantitative point of view, what can be detected looking at FIG. 4 is that the system code well predicts the edge channel temperatures (29, 26), while underestimates the inner channel ones (2, 5, 22). Such differences could be due to the limits of the presented models. Although, alternative (or complementary) explanations to these misalignments may also be the ones provided in [11] and related to the experimental setup: inhomogeneity in the pin power distribution and thermocouple mispositioning. Indeed, from a theoretical point of view, being 2 and 5 identical inner channels, no temperature difference should be detected among them (in contrast with what can be observed looking at the test data collected in FIG. 4). All these aspects must be furtherly analysed in the prosecution of the simulation activity. For this preliminary stage, the most important result is to identify what are the phenomena most influencing the thermal-hydraulic transient behaviour of liquid metal systems.

Finally, FIG. 5 reports the comparison between numerical and experimental results with respect to wall temperature. The system code predicts very well the test data, both qualitatively and quantitatively. For sake of brevity, the selected parameter is the one belonging to section C of channel 5. However, the above considerations can be extended to the other measured points. Following the conclusions drawn for the channel temperatures, **'wtm'** input deck was chosen as reference to plot the numerical results in FIG. 5. Nevertheless, it must be reminded that the HS block representing the electrically-heated rods is in common for all the models, as discussed in section 3.

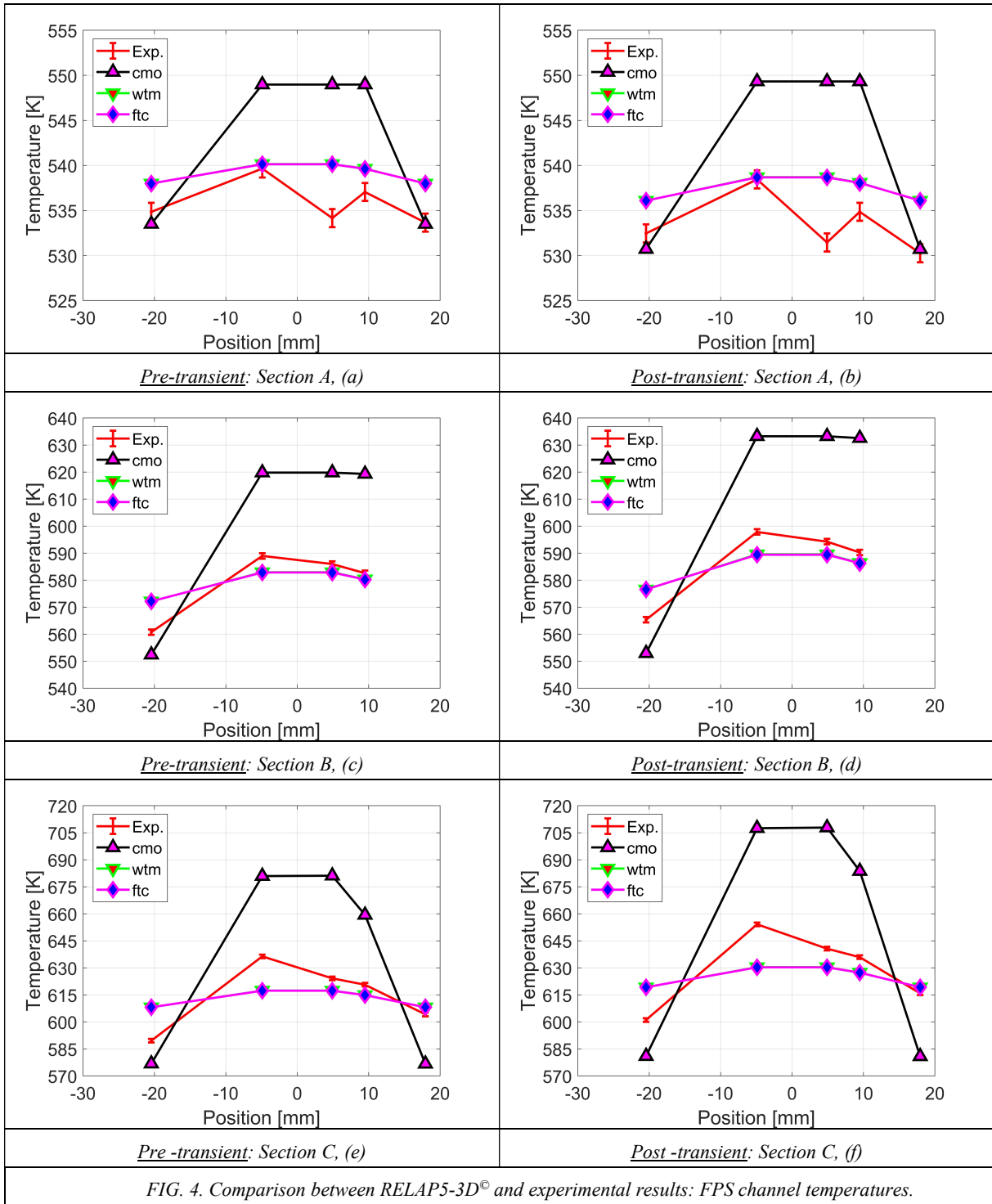


FIG. 4. Comparison between RELAP5-3D[®] and experimental results: FPS channel temperatures.

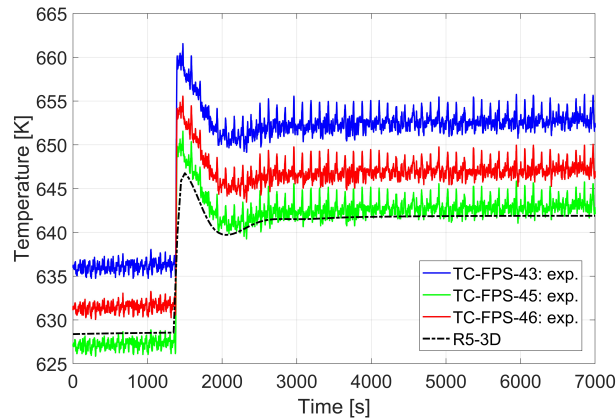


FIG. 5. Comparison between RELAP5-3D[®] and experimental results: wall temperature in channel 5 (section C), for ‘wtm’ input deck.

5. CONCLUSIONS

The goal of the paper is to preliminary evaluate the capability of RELAP5-3D[®] system code for subchannel analysis related to LFR applications. In this field, the adoption of a STH code could represent a good compromise between the features characterizing an ad hoc STH code and the ones corresponding to a full CFD code. Indeed, system codes are not affected by pre-set limitations (fuel geometries, type of coolant, etc.), in contrast with subchannel codes. In addition, even if they are not able to catch the 3D flow details characterizing a CFD simulation, they are suitable to investigate the system behaviour in transient and accidental conditions and to drastically reduce the computational time. However, this approach could not be appropriate for other applications, such as the evaluation of steady-state temperature field needed to assess corrosion effects. To verify the RELAP5-3D[®] capabilities, it was selected the experimental results coming from NACIE-UP facility hosted at ENEA Brasimone Research Centre. During 2017 test campaign a series of three fundamental tests was carried out. For the purposes of the current work, the first FT was chosen. To perform the comparison with empirical data, a complete RELAP5-3D[®] model of the facility was developed at DIAEE of Sapienza University of Rome. A special focus was given to the FPS modelling. Different input decks were prepared, characterized by growing complexity. The aim was to separately evaluate the impact of different phenomena on the simulation results. When only the cross-flow was taken into account (‘cmo’) a partial mixing occurs in the fuel bundle but it is not enough to flatten the temperature distribution as much as in the empirical observations. The introduction of the wire turbulent mixing had a deep impact on this aspect. The temperature profiles obtained as outcomes of ‘wtm’ input deck were always able to qualitatively reproduce the empirical acquisitions. Instead, the introduction of the fluid thermal conduction, ‘ftc’, had a negligible effect on the simulation results. Some issues arose when quantitatively comparing the numerical and experimental results. RELAP5-3D[®] underestimates the central channel temperatures. Even though this could be due to deficiencies of the presented models, alternative (or complementary) explanations of these misalignments can be found in the experimental setup, as suggested by previous studies present in literature. For what concerns the FPS global behaviour, the code well predicts the transient evolution both qualitatively and quantitatively. In the future developments of the simulation activity, the discrepancies observed with the test data will be furtherly investigated and the other experiments will be considered.

REFERENCES

- [1] Generation IV International Forum, Annual Report 2020. Available online: https://www.gen-4.org/gif/jcms/c_178286/gif-2020-annual-report.
- [2] GIF LFR Provisional System Steering Committee, Safety design criteria for Generation IV lead-cooled fast reactor system. LFR-SDC report, Rev. 1, 2021. Available online: https://www.gen-4.org/gif/jcms/c_176118/lfr-sdc-report-rev-1-march-2021.

- [3] Basehore, K.L., Todreas, N.E., SUPERENERGY-2: A Multiassembly Steady-State Computer Code for LMFBR Core Thermal-hydraulic Analysis. PNL-3379. Pacific Northwest Laboratory, Richland, WA, 1980.
- [4] Kim W.S., Kim Y.G., Kim Y.J., A subchannel analysis code MATRA-LMR for wire wrapped LMR subassembly. *Ann. Nucl. Energy* **29** (2002) 303-321. [https://doi.org/10.1016/S0306-4549\(01\)00041-X](https://doi.org/10.1016/S0306-4549(01)00041-X).
- [5] Liu X.J., Scarpelli N., Development of a sub-channel code for liquid metal cooled fuel assembly. *Ann. Nucl. Energy* **77** (2015) 425-435. <https://doi.org/10.1016/j.anucene.2014.10.030>.
- [6] Lodi F., Grasso G., Mattioli D., Sumini M., ANTEO+: A subchannel code for thermal-hydraulic analysis of liquid metal cooled systems. *Nucl. Eng. Des.* **301** (2016) 128-152. <https://doi.org/10.1016/j.nucengdes.2016.03.001>.
- [7] Wu D., Wang C., Gui M., Lan Z., Lu Q., Zhang D., Tian W., Qiu S., Su G.H., Improvement and validation of a sub-channel analysis code for lead-cooled reactor with wire spacers. *Int. J. Energ. Res.* **45** (2020) 12029-12046. <https://doi.org/10.1002/er.6015>.
- [8] Jeong J.H., Yoo J., Ha, K.S., Three-dimensional flow phenomena in a wire-wrapped 37-pin fuel bundle for SFR. *Nucl. Eng. Technol.* **47** (2015) 523-533. <https://doi.org/10.1016/j.net.2015.06.001>.
- [9] Chang S.K., Euh D.J., Choi H.S., Kim H., Choi S.R., Lee H.Y., Flow Distribution and Pressure Loss in Subchannels of a Wire-Wrapped 37-pin Rod Bundle for a Sodium-Cooled Fast Reactor. *Nucl. Eng. Technol.* **48** (2016) 376-385. <https://doi.org/10.1016/j.net.2015.12.013>.
- [10] Song M.S., Jeong J.H., Kim E.S., Numerical investigation on vortex behavior in wire-wrapped fuel assembly for a sodium fast reactor. *Nucl. Eng. Technol.* **51** (2019) 665-675. <https://doi.org/10.1016/j.net.2018.12.012>.
- [11] Pucciarelli A., Barone G., Forgiione N., Galleni F., Martelli D., NACIE-UP post-test simulations by CFD codes. *Nucl. Eng. Des.* **356** (2020) 110392. <https://doi.org/10.1016/j.nucengdes.2019.110392>.
- [12] Bieder, U., Graffard E., Qualification of the CFD code Trio U for full scale reactor applications. *Nucl. Eng. Des.* **238, 3**, (2008) 671–679. <https://doi.org/10.1016/j.nucengdes.2007.02.040>.
- [13] Memmott M., Buongiorno J., Hejzlar P., On the use of RELAP5-3D as a subchannel analysis code. *Nucl. Eng. Des.* **240** (2010) 807-815. <https://doi.org/10.1016/j.nucengdes.2009.11.006>.
- [14] The RELAP5-3D© Code Development Team, RELAP5-3D Code Manual Vol. I: Code Structure, System Models, and Solution Methods. INL/MIS-15-36723 Volume I, Revision 4.3, Idaho Falls, Idaho, USA, 2015.
- [15] Di Piazza I., Angelucci M., Marinari M., Tarantino M., Martelli D., Thermo-fluid dynamic transients in the NACIE-UP facility. *Nucl. Eng. Des.* **352** (2019) 110182. <https://doi.org/10.1016/j.nucengdes.2019.110182>.
- [16] Forgiione N., Martelli D., Barone G., Giannetti F., Lorusso P., Hollands T., Papukchiev A., Polidori M., Cervone A., Di Piazza I., Post-test simulations for the NACIE-UP benchmark by STH codes. *Nucl. Eng. Des.* **353** (2019) 110279. <https://doi.org/10.1016/j.nucengdes.2019.110279>.
- [17] Cheng S.K., Todreas N.E., Hydrodynamic models and correlations for bare and wire-wrapped hexagonal rod bundles – bundle friction factors, subchannel friction factors and mixing parameters. *Nucl. Eng. Des.* **92** (1986) 227-251. [https://doi.org/10.1016/0029-5493\(86\)90249-9](https://doi.org/10.1016/0029-5493(86)90249-9).
- [18] Chen S.K., Chen Y.M., Todreas N.E., The upgraded Cheng and Todreas correlation for pressure drop in hexagonal wire-wrapped rod bundles. *Nucl. Eng. Des.* **335** (2018) 356-373. <https://doi.org/10.1016/j.nucengdes.2018.05.010>.
- [19] V. Narcisi, C. Ciurluini, F. Giannetti, G. Caruso, Thermal-hydraulic transient analysis of the FFTF LOFWOS Test #13, *Nucl. Eng. Des.* **383** (2021) 111405. <https://doi.org/10.1016/j.nucengdes.2021.111405>.
- [20] Idelchik, I.E., Handbook of Hydraulic Resistance, second ed. Hemisphere Publishing Corporation, London (UK), 1986.
- [21] V. Narcisi, F. Giannetti, G. Caruso, Investigation on RELAP5-3D© capability to predict thermal stratification in liquid metal pool-type system and comparison with experimental data, *Nucl. Eng. Des.* **352** (2019) 110152. <https://doi.org/10.1016/j.nucengdes.2019.110152>.
- [22] Y.J. Yoo, P. Sabharwall, J.N. Reyes, O. Wu, J.J. Sienicki, Effects of fluid axial conduction on liquid metal natural circulation and linear stability. In: 2003 ANS/ENS International Winter Meeting, New Orleans, LA, pp. 1523–1530, 2003.
- [23] M.S. Kazimi and M.D. Carelli, Clinch River Breeder Reactor Plant Heat Transfer Correlation for Analysis of CRBRP Assemblies. CRBRP-ARD-0034, Westinghouse, Pittsburgh, PA, USA, 1976.
- [24] OECD/NEA Nuclear Science Committee, Handbook on Lead-bismuth Eutectic Alloy and Lead Properties, Materials Compatibility, Thermal-hydraulics and Technologies, 2015. Available online: <https://www.oecd-nea.org/science/pubs/2015/7268-leadbismuth-2015.pdf>.

- [25] P. Balestra, F. Giannetti, G. Caruso, A. Alfonsi, New RELAP5-3D lead and LBE thermophysical properties implementation for safety analysis of Gen IV reactors. *Sci. Tech. Nucl. Install.* **2016** (2016), 1687946. <https://doi.org/10.1155/2016/1687946>.